TENSILE MODULUS OF GLASS FIBER/CARBON FIBER REINFORCED POLYPROPYLENE HYBRID COMPOSITES FABRICATED BY VENTED INJECTION MOLDING

Xiaofei YAN[1], Lichao YU[2], Akio KATAOKA[3] and Hiroyuki Hamada[4]

[1] Department of Bio-based Materials Science, Kyoto Institute of Technology, Matsugasaki, Sakyo-ku, Kyoto, 606-8585, Japan, Email: xiaofei.yan@hotmail.com, web page: https://www.kit.ac.jp
[2] Department of Bio-based Materials Science, Kyoto Institute of Technology Matsugasaki, Sakyo-ku, Kyoto, 606-8585, Japan, Email: 591142637@qq.com, web page: https://www.kit.ac.jp/
[3] Nihon Yuki Co., Ltd., Sagamiharashi, 252-0203, Kanagawa, Japan, Email: a.kataoka@nihon-yuki.co.jp, web page: http://nihon-yuki.co.jp/
[4] The Future-Applied Conventional Technology Centre, Kyoto Institute of Technology, Matsugasaki, Sakyo-ku, Kyoto, 606-8585, Japan, Email: hhamada@kit.ac.jp, web page: https://www.kit.ac.jp/

Keywords: Tensile modulus, Direct fiber feeding injection molding, Carbon fiber, Glass fiber

ABSTRACT

This paper mainly discusses the elastic modulus of glass fiber/carbon fiber(GF/CF) reinforced polypropylene (PP) hybrid composites which fabricated by vented injection molding machine. The continuous carbon fiber roving strands are guided into the vent of the devolatilizing unit of injection barrel and fed into the melt by the shearing motion of the screw during plasticization process to make hybrid composites. The polypropylene-glass fiber pellets were fed through the hopper to avoid the serious fiber agglomeration phenomenon in the hybrid composites. The GF/PP composite were treated as a control. The scanning electron microscope (SEM) photos of the cross-section were used for observation the fiber status and to determine the boundary of skin-core structure of the composites. The fiber length and fiber orientation factor in the core layer and the skin layers of different composites were investigated to know the effect composites structure. The elastic modulus of composites manufactured by vented injection molding process was evaluated based on the laminate analogy approach method. The results were in good agreement with the experiment results in both glass fiber reinforced polypropylene composites and its carbon fiber reinforced polypropylene hybrid composite.

1 INTRODUCTION

Short fiber reinforced polymer (SFRP) composites fabricated by injection molding is widely used in automobiles, business machines, durable consumer items, sporting goods and electrical industries, etc. due to they are easier processing, cheaper and superior mechanical properties [1]. There is more than one-third of all thermoplastic materials are injection molded and more than half of all polymer processing equipment is for injection molding [2].

The vented injection molding has become popular those days because it has the most eye-catching advantages — no-bake the polymer pellets and it could save energy and production cost for company. It is now a new research hotspot that the fabrication of hybrid composites by feeding continuous long fiber bundle from the vented hole of vented injection molding machine. This process is called direct fiber injection molding (DFFIM) as it was shown in Figure1[3]. DFFIM is a fast, simple, and convenient way to manufacture the short fiber reinforced polymer composites. DFFIM means that the continuous fiber bundles were inserted from the vented hole of the injection molding machine which is typically used for releasing the volatile gasses of the hydroscopic materials. Therefore, it is not need to do compound of short or long fiber pellet and leads to a low cost. The continuous fiber roving strands are guided into the vent of the devolatilizing unit of injection barrel and fed into the melt by the shearing motion of the screw during plasticization process [4].

Meanwhile, hybrid composite is a hot topic in the composites material designs because it can make the full use of material and it can find the balance between the advantage and disadvantage of two or more material [5]. The advantage of one type of material could complement with what are lacking in

other fiber or matrix and the cost of composites material would be also decrease [6]. And hybrid composite which made by glass fiber (GF), carbon fiber (CF) and polypropylene (PP) is popular those days especially in automobile industry such as fan blades of engine cooling system, dashboard, door, front-end module frame and so on. And it makes the full use of all the properties of those materials.

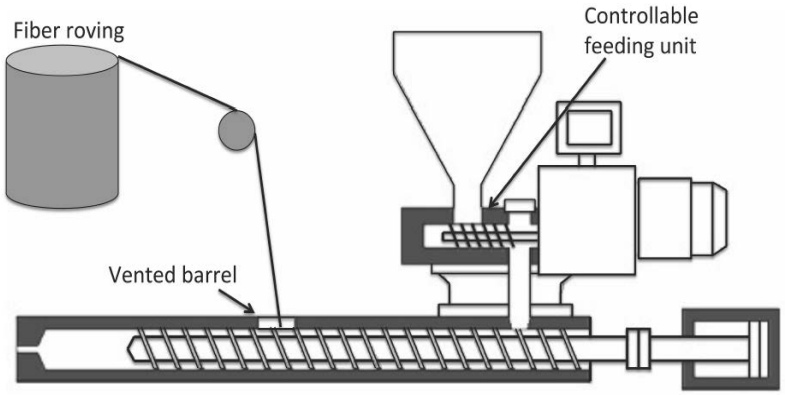

Figure 1: Schematic illustration of the DFFIM technology. [3]

The elastic modulus is a very important parameter that has important effect on the application area of composite materials. A lot of research work on the tensile modulus of SFRPs has been done by other researchers. The Cox shear lag model developed in 1952 is the pioneering work for predicting the modulus of unidirectional short fiber reinforced polymer materials [7]. Halpin and Tsai (1967) used semi-empirical approaches to derive the elastic modulus of unidirectional fiber composites [8]. Tsai and Hahn et al. have developed the inverse rule of mixtures (iRoM) equation to predict the transverse modulus of unidirectional continuous fiber composites [9]. Fu et al. (1998) created a model to determine the transverse modulus of SFRP composites [10]. Lavengood and Gottler (1971) used approximate averaging methods to invent a rule-of-thumb expression for the modulus of a structure with a 2-dimensional fiber orientation [11]. Jayaraman et al. (1996) have established the paper physics approach (PPA) to predict the elastic modulus of SFRP composites which considered the fiber orientation and fiber length distributions. However, the experimental results are not in agreement with the predictions [12]. Xia et al. (1995) applied the laminate analogy approach (LAA) methods to predict the stiffness of SFRPs and some of their results were not satisfactory [13]. S. Fu et al. (2009) compared all the aforementioned models and found that LAA is suitable for predicting the elastic modulus of SFRP composites. For hybrid composites, the Young's modulus was also predicted by the rule of hybrid mixtures (RoHM) [14].

The papers mainly discussed the tensile modulus of glass fiber/carbon fiber reinforced polypropylene hybrid composites which fabricated by DFFIM process. The fiber length and fiber orientation in the core layer and skin layers were investigated. The scanning electron microscope (SEM) photos of the cross-section were used for observing the fiber status and the boundary of skin-core structure of the composites. The elastic modulus of composites was evaluated based on the laminate analogy approach method.

2 THEORY

The simulated process of the laminated plated model of a 3-dimensional SFRP is illustrated in Fig. 2 [14]. It is considered that the SFRP has only a planar fiber orientation distribution (see Fig. 2(b)). The resulting composite is regarded as the combination of many laminates according to fiber length distributions. Each laminate has the same fiber length (see Fig. 2(c), in which '$L(l_i)$, i=1, 2, …, n' means the i^{th} laminate with the same fiber length l_i). Each laminate with the same fiber length is then treated as a stacked sequence of laminates which have the same fiber length and fiber orientation (see Fig. 2(d), in which '$L(l_i, \theta_j)$, j=1, 2, …, m' means the j^{th} laminate with the same fiber length l_i and the same fiber orientation angle θ_j). The Young's modulus or tensile strength of the real SFRP can be

obtained by analyzing the modulus or tensile strength of all those laminates. It is considered that the fiber lengths between *l* and *l*+d*l* and fiber orientation angles between θ and θ+dθ are in the same ply.

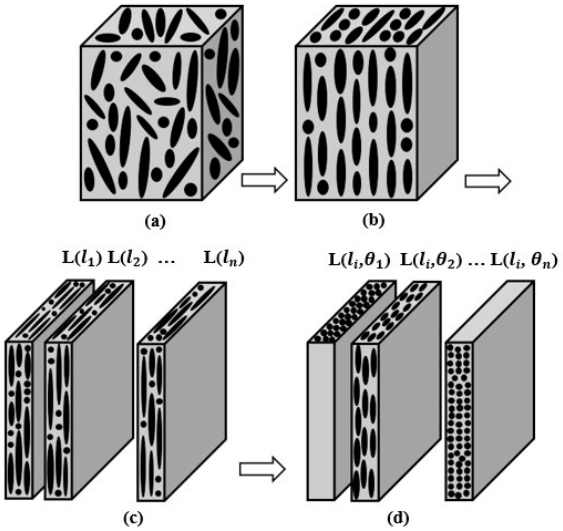

Figure 2: Schematic the laminated plate model of a 3D short-fiber-reinforced polymeric composite: (a) the real 3D SFRP, (b) the imagined SFRP, (c) the imagined SFRP is considered as a combination of laminate each laminate is treated as a stacked sequence of laminates, each laminate having the same fiber length and (d) each laminate is treated as a stacked sequence of laminates, each laminate having the same fiber length and the same fiber orientation. [14]

For aligned short-fiber composites, the longitudinal modulus, E_{11}, depends on the fiber aspect ratio (l/d). According to the Cox shear-lag model, E_{11} is given by equation (1) [7]:

$$E_{11} = E_f\left[1 - \frac{tanh(\beta l/2)}{\beta l/2}\right]V_f + E_m(1 - V_f) \quad (1)$$

Where E_f and E_m are the elastic modulus of the fibers and the elastic modulus of the matrix, respectively. V_f is the fiber volume fraction, and β is given by equation (2) [7]:

$$\beta = \left[\frac{2\pi G_m}{E_f(\pi {r_f}^2)\ln(R/r_f)}\right]^{1/2} \quad (2)$$

Where G_m is the shear modulus of the matrix and R is the mean separation of the fibers normal to their length, and r_f is the fiber radius.

For a hexagonal fiber packing arrangement,

$$\ln\left(\frac{R}{r_f}\right) = \frac{1}{2}\ln\left(\frac{2\pi}{\sqrt{3}V_f}\right) \quad (3)$$

For a square packing arrangement,

$$\ln\left(\frac{R}{r_f}\right) = \frac{1}{2}\ln\left(\frac{\pi}{V_f}\right) \quad (4)$$

The transverse modulus and the in-plane shear modulus, E_{22} and G_{12}, are almost independent of fiber aspect ratio. In this investigation, we use the Halpin-Tsai equations [8, 9]:

$$E_{22} = E_m(1 + 2\eta_1 V_f)/(1 - \eta_1 V_f) \quad (5)$$

$$G_{12} = G_m(1 + 2\eta_2 V_f)/(1 - \eta_2 V_f) \quad (6)$$

Where

$$\eta_1 = \left(\frac{E_f}{E_m} - 1\right)/\left(\frac{E_f}{E_m} + 2\right) \quad (7)$$

$$\eta_2 = (\frac{G_f}{G_m} - 1)/(\frac{G_f}{G_m} + 1) \tag{8}$$

Where G_f is the fiber shear modulus.

The longitudinal Poisson's ratio,v_{12}, is calculated by the rule of mixtures:

$$v_{12} = v_f V_f + v_m(1 - V_f) \tag{9}$$

where v_f and v_m are the Poisson's ratios of the fibers and matrix, respectively. The transverse Poisson's ratio,v_{21}, can be expressed as:

$$\mathrm{v_{21}} = \mathrm{v_{12}E_{22}/E_{11}} \tag{10}$$

It calculates the components of the stiffness matrix, Q_{ij}, that relates the stress to the strain for the uniaxial ply when the principal stress directions are aligned with the principal fiber directions [14]:

$$\begin{Bmatrix}\sigma_1\\ \sigma_2\\ \tau_{12}\end{Bmatrix} = \begin{Bmatrix}\mathrm{Q_{11}} & \mathrm{Q_{12}} & \mathrm{Q_{16}}\\ \mathrm{Q_{12}} & \mathrm{Q_{22}} & \mathrm{Q_{26}}\\ \mathrm{Q_{16}} & \mathrm{Q_{26}} & \mathrm{Q_{66}}\end{Bmatrix}\begin{Bmatrix}\varepsilon_1\\ \varepsilon_1\\ \gamma_{12}\end{Bmatrix} \tag{11}$$

Where

$$Q_{11} = E_{11}/(1 - v_{12}v_{21}) \tag{12}$$
$$Q_{12} = v_{21}Q_{11} \tag{13}$$
$$Q_{16} = 0 \tag{14}$$
$$Q_{22} = E_{22}/(1 - v_{12}v_{21}) \tag{15}$$
$$\mathrm{Q_{26}} = 0 \tag{16}$$
$$Q_{66} = G_{12} \tag{17}$$

The stress–strain relation in the off-axis system is given by:

$$\begin{Bmatrix}\sigma_1'\\ \sigma_2'\\ \tau_{12}'\end{Bmatrix} = \begin{Bmatrix}Q_{11}' & Q_{12}' & Q_{16}'\\ Q_{12}' & Q_{22}' & Q_{26}'\\ Q_{16}' & Q_{26}' & Q_{66}'\end{Bmatrix}\begin{Bmatrix}\varepsilon_1'\\ \varepsilon_2'\\ \gamma_{12}'\end{Bmatrix} \tag{18}$$

The transformation equation between the components of the stiffness matrix in the on-axis system and the off-axis system is:

$$\begin{Bmatrix}Q_{11}'\\ Q_{22}'\\ Q_{12}'\\ Q_{66}'\\ Q_{16}'\\ Q_{26}'\end{Bmatrix} = \begin{pmatrix} c^4 & s^4 & 2c^2s^2 & 4c^2s^2\\ s^4 & c^4 & 2c^2s^2 & 4c^2s^2\\ c^2s^2 & c^2s^2 & c^4+s^4 & -4c^2s^2\\ c^2s^2 & c^2s^2 & -2c^2s^2 & (c^2-s^2)^2\\ c^3s & -cs^3 & cs^3-c^3s & 2(cs^3-c^3s)\\ cs^3 & -c^3s & c^3s-cs^3 & 2(c^3s-cs^3)\end{pmatrix}\begin{Bmatrix}Q_{11}\\ Q_{22}\\ Q_{12}\\ Q_{66}\end{Bmatrix} \tag{19}$$

Where $c = \cos\theta$ and $s = \sin\theta$.

The transformed stiffness constants, Q_{ij}', are integrated through the thickness of the laminate to obtain the overall laminate stiffness matrix, $\overline{A}_{ij}$:

$$\mathrm{\overline{A}_{ij} = \sum_{k=1}^{M} Q_{ij}^{'} h_k} \tag{20}$$

Where *M* represents the number of plies in the laminate; k is the serial index of the ply in the laminate; and h_k is the thickness fraction of the k[th] ply.

Since the imagined SFRP composite has a continuous fiber orientation distribution and a continuous fiber length distribution, then, as described above, the k[th] ply can be considered to contain fibers of the length between l and l+dl and orientation between θ and θ+dθ. Thus, the summation in equation (20) must be replaced by the corresponding integral:

$$\overline{A}_{ij} = \int_{l_{min}}^{l_{max}} \int_{\theta_{min}}^{\theta_{max}} Q_{ij}' f(l) g(\theta) dl d\theta \tag{21}$$

where $0 \le l_{min} \le l \le l_{max} < \infty$ and $0 \le \theta_{min} \le \theta \le \theta_{max} \le \pi/2$. The engineering tensile stiffness is obtained from the laminate stiffness components:

$$\overline{E}_{11} = \frac{\overline{A}_{11}\overline{A}_{22} - \overline{A}_{12}^2}{\overline{A}_{22}} \tag{22}$$

$$\overline{E}_{22} = \frac{\overline{A}_{11}\overline{A}_{22} - \overline{A}_{12}^2}{\overline{A}_{11}} \tag{23}$$

$$\overline{G}_{12} = \overline{A}_{66} \tag{24}$$

$$\overline{v}_{12} = \overline{E}_{11}\frac{\overline{A}_{12}}{\overline{A}_{11}\overline{A}_{12} - \overline{A}_{12}^2} = \frac{\overline{A}_{12}}{\overline{A}_{22}} \tag{25}$$

$\overline{E}_{11}$ is the elastic modulus of the imagined SFRP composite with a planar fiber orientation distribution g(θ) and fiber length distribution $f(l)$. While other expressions for $\overline{E}_{22}$, $\overline{G}_{12}$, and $\overline{v}_{12}$ hold true only for the imagined SFRP.

3 EXPERIMENT DETAILS

3.1 Materials

Polypropylene (PP) pellets (Grade: Y101S, melt flow rate=15g/10min, density=0.9g/m^3, Sumitomo Chemical Co., Ltd., Japan.) were used for dilution glass fiber-polypropylene pellets and making polypropylene-carbon fiber composites.

Pre-compounded glass fiber-polypropylene (GF/PP) pellets (Grade: GWH42, Sumitomo Chemical Co., Ltd., Japan.) with 25wt.% mass fraction were diluted by polypropylene pellets to change the glass fiber content to 10wt.%. The polypropylene used in the GFPP pellets is the same with PP pellets.

The carbon fibers (CF) (Grade: TR50S 6L, 6000 fibers/bundle, diameter of each fiber is 7μm) from Mitsubishi Rayon Co, Ltd, Japan were used as the hybrid fiber to feed into the vented hole of injection molding machine. The detail information of materials was listed in Table 1.

Table 1 Physical parameters of the materials

Material	Longitudinal modulus (GPa)	Transverse modulus (GPa)	Shear modulus (GPa)	Poisson ratio	Density (g/cm^3)	Diameter (μm)
Polypropylene	1.6	1.6	0.6	0.35	0.946	—
Glass fiber	74	74	30	0.25	2.54	13
Carbon fiber	240	15	50	0.3	1.82	7

3.2 Preparation of the specimen

A 75T (SE75-DUZ-C110 φ28, Sumitomo Heavy Industries, Ltd.) injection molding machine was refitted and used for making the specimens. PP pellets were mixed together with GF/PP pellets to dilute the GF mass fraction to 10wt.%, the mixed pellets were fed at a stable speed through the hopper. CF roving was guided into the vent of the devolatilizing unit of the barrel and fed into the melt by the shearing action of the screw during the plasticization process to make GF/CF/PP hybrid composites. All the specimens were injection molded into dumbbell-shaped tensile bars. The thickness and width of the specimens are 4 mm and 10 mm, respectively. The feeding speed and charging speed were 50 r/min and 135 rpm, respectively. The barrel temperature was set from 240℃ to 200℃ while the mold temperature was set at 30℃. The speed of the plasticization screw was 180 rpm. GF/PP composites and CF/PP composites which were manufactured in same conditions by no-inset CF and only PP was fed through the hopper were treated as a control, respectively. Detail information of the specimen is shown in Table 2.

Table 2 Composition of Composites

Specimen	Composition	Method
GF/PP composite	GFPP	GFPP was fed from hopper
GF/CF/PP composite	GFPP + CF	GFPP was fed from hopper, CF was inset from vent hole

3.3 Method

3.3.1 Scanning electron microscopy photos of fracture surface

Fracture surfaces of the specimens were observed by scanning electron microscopy (SEM, JSM-5200 JEOL Japan Electronics Co., Ltd.). Prior to the SEM observations, all fracture surfaces of the tensile specimens were sputter coated with gold to avoid electrical charging during examination.

3.3.2 Fiber length measurement

For GF/PP composites, fiber samples are collected by burning off PP in a muffle furnace at 600℃ for 6 hours in air according to ASTM D3171-15. While for the GF/CF/PP hybrid composite, the samples are placed in the furnace for 1 hour at 600℃ to burn off PP. The fibers were cast onto glass slides and dispersed in natural water. The fiber dispersion is then dried, leaving an even fiber distribution. Optical photographs were taken of the fiber samples, and the photos were processed with Adobe Photoshop CC in order to mark the fiber length. ImageJ was then used to measure the fiber length. The carbon fibers and glass fibers were distinguished by color - the carbon fibers appearing black, and the glass fibers appearing a pale yellow.

3.3.3 Fiber orientation measurement and fiber volume fraction

The specimens were embedded into epoxy resin. After the epoxy resin cured for 18 hours, the specimens were ground and polished and prepared for taking optical microscopy images of the cross-section. The images were first processed with Adobe Photoshop CC to make the fibers, and then ImageJ was used to measure the fiber orientation angles, the probability density distribution, and the fiber orientation factor.

The fiber volume fraction in each layer was calculated by making the summary of the area of fibers in each layer according to the full cross-section scale of specimen.

3.3.4 Tensile test

The tensile properties of the specimens were determined by using a universal testing machine (55R 4206, Instron Co., Ltd.) at a constant crosshead speed of 1 mm/min, using five samples for each measurement. An extensometer (Instron Co., Ltd) with a gauge length of 50 mm was used for the strain measurements. It was operated according to ASTM D638.

4 RESULTS AND DISCUSSION

4.1 Scanning electron microscopy of the fracture surface

The fracture surface of composites after tensile experiment was presented in Figure 3. It can be clearly seen from Fig. 2 that all the composites have shown the skin-core-skin structure. The core layers have shown more trend to be array to transverse direction than the skin layers.

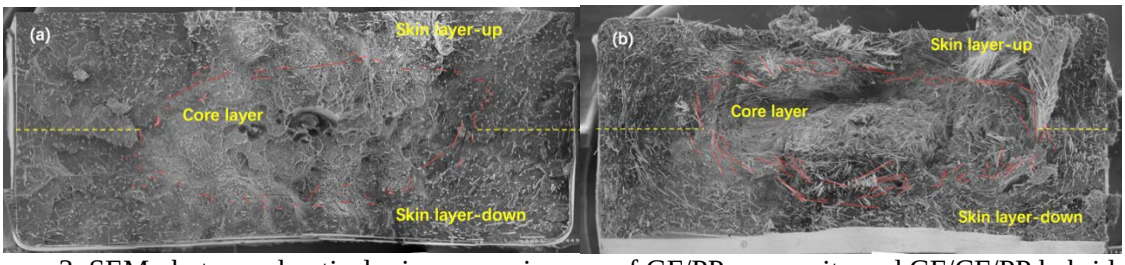

Figure 3: SEM photos and optical microscopy images of GF/PP composite and GF/CF/PP hybrid composites: (a) GF/PP composite; (b) GF/CF/PP hybrid composite. (Red line is the boundary of the core layer and the skin layers)

The fibers dispersion status of hybrid composite seem to be non-uniform distributed along the cross-section of the specimen especially in the core layer. Both hybrid composite and GF/PP composite are shown a number of transverse orientation at the skin layers. The GF/PP composite has more tendency to be orientated in the flow direction than GF/CF/PP hybrid specimen. The hybrid composite has fiber agglomeration phenomenon where there has little or no matrix between fibers, the fibers are directly close with each other while the GF/PP composite does not show such phenomenon. This could greatly

influence the mechanical properties of hybrid composites. The fiber agglomeration areas are mainly dispersed in the core layer.

4.2 Fiber length, fiber orientation and fiber volume fraction

For GF/PP composite and hybrid composite, the fiber length information were presented in Figure 4 and Table 3. The glass fiber in the core layer is a little shorter than in the skin layers and it is due to the higher shear rate of in the core layer of GF/PP composites.

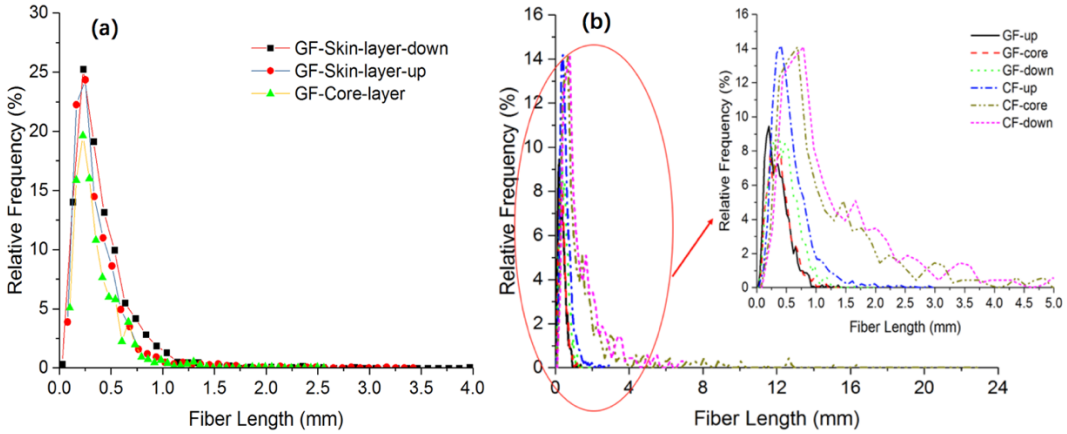

Figure 4: Fiber length in composites: (a) GF/PP composite; (b) GF/CF/PP hybrid composite.

It can be known that the carbon fiber fed through the vented hole is much longer and the longest could reach as long as 16.321 mm. It reveals that the DFFIM process is an effect way to get longer fiber composites. For hybrid composite, the carbon fiber in the core layer is longer than in the skin layers while the glass fiber shows the same trend in the GF/PP composite. The fluidity of longer carbon fiber in the melted polypropylene is poor and it weaken the fountain effect, it is the main reason for carbon fiber agglomeration phenomenon, the entangled long carbon fibers further hinder the regularity of fiber dispersion.

Table 3 Fiber length in composites

Composites	Fiber	Layer	Maximum Fiber Length (mm)	Minimum Fiber Length (mm)	Average Fiber Length (mm)	Standard Deviation (mm)
GF/PP composite	GF	Up	3.466	0.036	0.385	0.292
		Core	2.590	0.069	0.362	0.245
		Down	3.969	0.027	0.409	0.290
Hybrid composite	GF	Up	1.287	0.047	0.394	0.195
		Core	1.366	0.053	0.358	0.196
		Down	1.900	0.058	0.471	0.237
	CF	Up	2.864	0.060	0.567	0.330
		Core	16.312	0.199	1.614	2.080
		Down	6.023	0.057	0.589	0.519

The fiber orientation angle distribution of different fiber in different layers in different composites is presented in Figure 5. The fiber orientation coefficient (f_θ) and fiber volume fraction are shown in Table 4. The volume fraction of glass fiber in the skin layers is higher than that in the core layer no matter in GF/PP composite or hybrid composite. It indicates that the glass fiber has more tendency to distribute in skin layers while carbon fiber has shown opposite results. The carbon fiber tends to dispersion in the core layer in the DFFIM composites.

The fibers orientated has more preference to be arrayed to the flow direction in the skin layers and the fibers in the core layer trends to be disposed along the transverse direction in the GF/PP composite. The fiber orientation coefficient in the core layer of GF/CF/PP hybrid composite is higher than that in the skin layers. The carbon fiber is not dispersion good enough in the composite as the fiber bundle exist

in the final specimen. Some of fiber bundles arrayed to the flow direction will significantly improve the orientation coefficient.

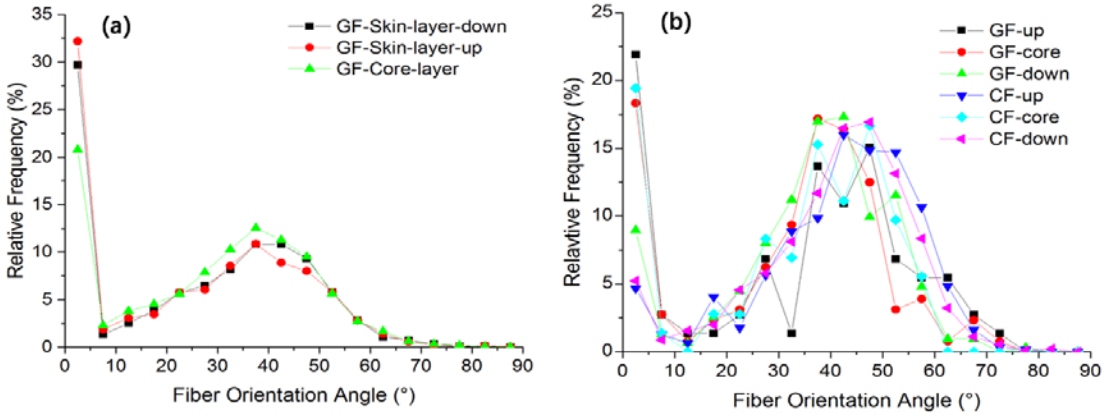

Figure 5: Fiber orientation in composites: (a) GF/PP composite; (b) GF/CF/PP hybrid composite.

Table 4 Fiber orientation coefficient and fiber volume fraction in different layers

Composites	Fiber	Layer	Fiber orientation coefficient (f_θ)	v_f(%)
GF/PP composite	GF	Up	0.616	4.129
		Core	0.558	3.927
		Down	0.598	4.097
Hybrid composite	GF	Up	0.472	3.305
		Core	0.495	3.101
		Down	0.477	3.314
	CF	Up	0.339	2.516
		Core	0.426	3.312
		Down	0.357	2.421

4.3 Elastic modulus of composites

The predication results of flexural modulus for GF/PP composites and GF/CF/PP hybrid composites were presented in Table 3. It can be seen that the modulus difference in the core layer and skin layers was small in GF/PP composite. The predicated modulus in the core layer of hybrid composite is higher than that of skin layers. The predicated modulus based on the laminate analogy approach method were in good agreement with the experiment results.

Table 3 Predicated flexural modulus results

Composites	Layer	Predicated Modulus (GPa)	Experiment Modulus	
			(GPa)	CV (%)
GF/PP composite	Up	3.758	3.703	0.097
	Core	3.721		
	Down	3.782		
	Average	3.754		
GF/CF/PP composite	Up	7.824	7.769	1.216
	Core	8.034		
	Down	7.835		
	Average	7.898		

5 CONCLUSIONS

The paper mainly discussed the modulus of GF/PP composite and hybrid composite based on the laminate analogy approach method. The modulus of core layer and skin layers were investigated, respectively. The following conclusions were obtained:

1) DFFIM is an effect way to increase fiber length in the composite and fiber feeding through the vented hole is much longer. Glass fiber has more tendency to be arrayed in the skin layers in GF/PP composite and hybrid composite while carbon fiber tends to dispersion in the core layer in the hybrid composites. The dispersion of glass fiber shows relative evenly distribution.

2) The predicated modulus was in good agreement with the experiments for both the glass fiber reinforced polypropylene composite and its hybrid composite. The modulus in the core layer of hybrid composite was larger than that of skin layers. The modulus difference of skin layers and core layer was small in the GF/PP composite.

ACKNOWLEDGEMENTS

This work was financial supported under the State Scholarship Fund [Award N0.: 201506630020] by the China Scholarship Council which is a non-profit institution affiliated with the Ministry of Education of the People's Republic of China.

REFERENCES

[1] Shao-Yun Fu, Bernd Lauke and Yiu-Wing Mai, *Introduction to short fibre reinforced polymer composites*, Science and engineering of short fibre reinforced polymer composites, Woodhead Publishing Limited, Cambridge, 2009.

[2] Osswald T.A. and Hern´andez-Ortiz J.P. Polymer processing: modeling and simulation, Hanser Gardner Publications, Munich, 2006.

[3] Yan, X., Yang, Y. and Hamada, H., Tensile properties of glass fiber reinforced polypropylene composite and its carbon fiber hybrid composite fabricated by direct fiber feeding injection molding process. *Polymer Composites*, 2017. (doi: 10.1002/pc.24378).

[4] Yan X, Uawongsuwan P, Murakami M, Imajo A, Yang Y, Hamada H. Tensile Properties of Glass Fiber/Carbon Fiber Reinforced Polypropylene Hybrid Composites Fabricated by Direct Fiber Feeding Injection Molding Process. *ASME. ASME International Mechanical Engineering Congress and Exposition*, **Volume 2: Advanced Manufacturing**, 2016, pp. V002T02A045. (doi: 10.1115/IMECE2016-66270).

[5] Putinun Uawongsuwan, Structure and properties of short fiber reinforced polymer composite and hybrid composite fabricated by injection molding process, *Ph.D. dissertation, Dept. Adv. Fib. Sci., Kyoto Inst. Tech.*, Kyoto, Japan, 2014.

[6] Manders P W, Bader M G, The strength of hybrid glass/carbon fibre composites, *Journal of Materials Science*, **16** (8), 1981, pp. 2233-2245 (doi: 10.1007/BF00542386).

[7] Cox H L., The elasticity and strength of paper and other fibrous materials, British Journal of Applied Physics, **3**(3), 1952, pp. 72-79 (doi: 10.1088/0508-3443/3/3/302).

[8] Halpin J C, Tsai S W, Environmental factors in composite materials design. US Air Force Materials Lab. Rep. AFML Tech Rep, 1967, pp. 67–423.

[9] Tsai S W, Hahn H T. Introduction to composite materials, Technomic, Lancaster, PA, 1980.

[10] Fu S Y, Hu X, Yue C Y., A New Model for the Transverse Modulus of Unidirectional Fiber Composites, *Journal of Materials Science*, **33** (20): 1988, pp. 4953 (doi: 10.1023/A:1004442520797).

[11] Lavengood R E, Goettler L A, Stiffness of non-aligned fiber reinforced composites. US Government R&D Reports, AD886372, National Technical Information Service, Springfield, VA., 1971.

[12] Jayaraman K, Kortschot M T., Correction to the Fukuda-Kawata Young's modulus theory and the Fukuda-Chou strength theory for short fibre-reinforced composite materials, *Journal of Materials Science*, **31** (8), 1996, pp. 2059 (doi: 10.1007/BF00356627).

[13] Xia M, Hamada H, Maekawa Z, Flexural stiffness of injection molded glass fiber reinforced thermoplastics. *International Polymer Processing*, **10**(1), 1995, pp.74-81(doi: 10.3139/217.950074).

[14] Fu, S. Y., Xu, G., & Mai, Y. W., On the elastic modulus of hybrid particle/short-fiber/polymer composites. *Composites Part B: Engineering*, **33**(4), pp. 291-299 (doi: 10.1016/j.compscitech.2008.10.020).